

# TENSILE RESIDUAL STRESS FIELDS PRODUCED IN AUSTENITIC ALLOY WELDMENTS

Douglas J. Hornbach and Paul S. Prév y  
Lambda Research

## ABSTRACT

Residual stresses developed by prior machining and welding may either accelerate or retard stress corrosion cracking (SCC), in austenitic alloys, depending upon their magnitude and sign. A combined x-ray diffraction (XRD) and mechanical technique was used to determine the axial and hoop residual stress and yield strength distributions into the inside diameter surface of a simulated Alloy 600 penetration J-welded into a reactor pressure vessel. The degree of cold working and the resulting yield strength increase caused by prior machining and weld shrinkage were calculated from the line broadening distributions. Tension as high as +700 MPa was observed in both the axial and hoop directions at the inside diameter adjacent to the weld heat affected zone (HAZ). Stresses exceeding the bulk yield strength develop due to the combined effects of cold working of the surface layers during initial machining, and subsequent weld shrinkage. Cold working produced by prior machining was found to influence the final residual stress state developed by welding.

**Keywords:** residual stress, stress corrosion cracking, machining, welding, Alloy 600

## INTRODUCTION

Stress corrosion cracking has been observed for decades in austenitic alloy weldments such as type 304 stainless steel and Alloy 600. Maintaining pressurized and boiling water reactors continues to be a key concern. Intergranular SCC was observed in several partial J-weld penetrations of both heater sleeve and pressurizer nozzles in nuclear pressure vessels (Hall and Scott, 1989). Initial investigations of Alloy 600 sleeves and nozzles prior to welding indicated that the residual stresses produced by machining alone were well below the threshold stress level of +276 MPa (Gorman, 1986) required to initiate stress corrosion cracking.

A series of J-weld mockup specimens consisting of Alloy 600 tubular sleeves welded into a steel block were prepared to simulate the combined effects of machining and welding which occur during fabrication of pressure vessel penetrations. A mechanical strain gauging and x-ray diffraction technique was utilized to expose the inside diameter surface and allow for measurement of both the macroscopic residual stress and the degree of cold working of the surface. Preliminary results obtained with relatively coarse depth resolution show a pronounced change in the magnitude of residual stress and cold work with increasing depth into the surface of the sample (Hall, et al., 1993, Hall, et al., 1994). The purpose of the current investigation was to characterize the residual stress and cold working with higher depth and spatial resolution than was initially acquired.

## SPECIMEN FABRICATION

Several J-weld heater sleeve mockups were prepared by ABB-Combustion Engineering to simulate as accurately as possible the actual fabrication procedures used in the pressure vessel penetrations which had experienced stress corrosion cracking in service. Mockup specimen #9, which was prepared with a 50 deg. penetration angle, was used in this investigation. The Alloy 600 heater sleeve was taken from decontaminated material removed from a reactor system which had experienced SCC failure. Portions of the inside surface of the sleeve had been reamed during the original pressure vessel fabrication. The use of portions of decontaminated sleeves ensured that the residual stress and cold work distributions produced by reaming of the sleeves would be identical to the sleeves which experienced field failures.

A massive carbon steel block nominally 152 mm square at the base was machined from archival SA-533B reactor vessel steel with a 50 deg. penetration angle as shown in Fig. 1. The surface was overlaid with Alloy 82 weld metal to a nominal depth of 10 mm. The penetration clearance hole was drilled down the

axis of the block, and J-weld preparations were machined into the Alloy 82 overlay. The Alloy 600 sleeve was then inserted into the block and welded in place with Alloy 82 filler metal using the same welding parameters and bead deposition sequence prescribed for the original sleeves which had experienced SCC.

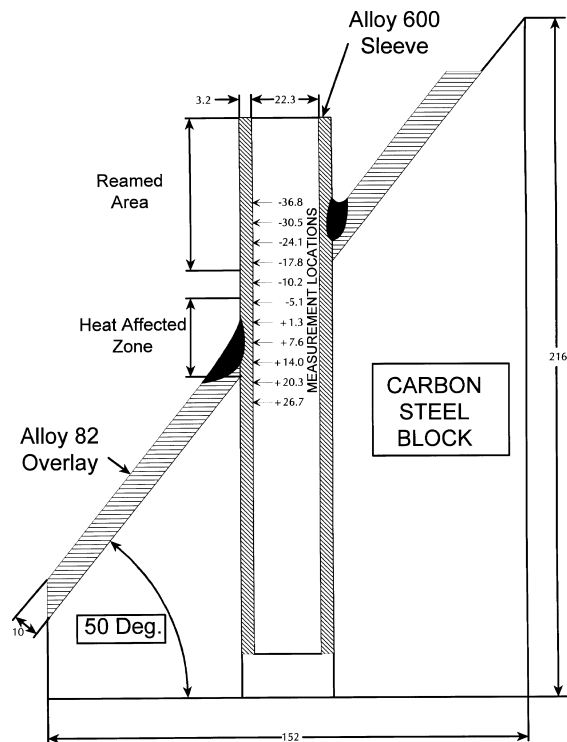


**Fig. 1** - Alloy 600 50 deg. heater sleeve penetration J-weld mockup specimen geometry.

## EXPERIMENTAL TECHNIQUE

The weld mockup was sectioned axially to provide access for measurement by XRD on the inside diameter of the Alloy 600 sleeve. The mockup was sectioned along a plane perpendicular to Fig. 1, which exposed the "high" and "low" side weld regions, where most of the field failure SCC had occurred. The XRD measurement locations shown in Fig. 1 are defined by the axial displacement from the intersection of the plane defining the top surface of the Alloy 82 overlay and the inside diameter surface of the Alloy 600 sleeve on the low (left) side. These coordinates are used for the presentation of all data obtained on the inside diameter surface in order to maintain reference to the location of the weld.

The stress relaxation on the I.D. was monitored through six biaxial strain gages spanning nominally 64 mm. The residual strain relaxations at each XRD measurement location were interpolated along the inside surface between the center points of the strain gage grids. The high side had been used for one of the previous studies (Hall, et al., 1993).

After sectioning, the strain gages were removed chemically from the inside diameter surface, and XRD residual stress measurements were made in both the hoop and axial directions at the measurement locations shown in Fig. 1. Layers of material were then electropolished from the inside surface, and the process repeated to a total depth of nominally 0.25 mm into the inside surface of the sleeve. The diffraction peak width and residual stress distributions were measured simultaneously as functions of depth.

X-ray diffraction residual stress measurements were made employing a  $\sin^2\psi$  technique and the diffraction of Mn or Cu  $K\alpha$  radiation from the (311) or (420) planes of the austenitic alloy (Hilley, 1971, Noyan and Cohen, 1987, Cullity, 1978, Prev y, 1986a). The Cu  $K\beta$  and Fe and Cr  $K\alpha$  fluorescent background radiation was suppressed using a high energy resolution solid state Si(Li) detector and single channel analyzer. The x-ray elastic constants required to calculate the macroscopic residual stress from the strain measured in the (311) and (420) directions were determined empirically (Prev y, 1977) in accordance with ASTM E-1426. Systematic errors due to diffractometer and sample misalignment were monitored in accordance with ASTM E-915. The position and width of the  $K\alpha_1$  diffraction peak was separated from the combined  $K\alpha$  doublet using Pearson VII function peak profile deconvolution (Prev y, 1986b).

Previous studies of the nickel base super-alloys Inconel 718 and Rene 95, and the stress corrosion resistant Alloys 690 and 600 had shown that an empirical relationship could be established between the  $K\alpha_1$  peak width and the degree to which the material was cold worked (Prev y, 1987, Prev y, 1981). If the measure of cold work is taken to be the true plastic strain, then the total line broadening is found to be independent of the mode of deformation, whether tensile or compressive, and to be accumulative for complex deformation histories (Prev y, 1987). The dependence on the Mn  $K\alpha$  (311) diffraction peak on true plastic strain is shown in Fig. 2.

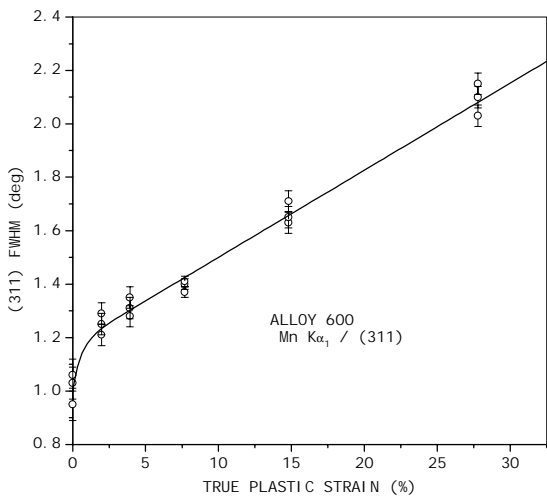


**Fig. 2** - Empirical relationship between (311) peak width and cold work (true plastic strain) for Alloy 600.

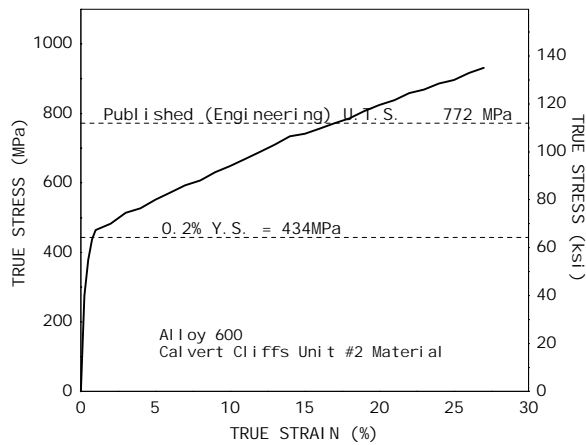


**Fig. 3** - True stress-strain curve measured for Alloy 600 heater sleeve material removed from service.

The yield strength increase associated with the amount of cold working at each measurement location and depth was estimated using a true stress-strain curve from the equivalent true plastic strain. The tension true stress-strain curve for the Alloy 600 material involved in the field failures is presented in Fig. 3 to nominally 27% strain. The bulk yield strength is nominally 434 MPa, and approximately doubles when the alloy is cold worked 25%, as seen in Fig. 3. As shown in the results obtained, the amount of cold work induced in machining Alloy 600 can readily exceed the nominally 27% cold work achieved in tension to produce the data in Fig. 3. It was therefore necessary to extrapolate to estimate yield strengths beyond the range of the true stress-strain curve obtained in tension. The ultimate tensile strength (UTS) will also increase with prior cold work. The published (engineering) UTS (Alloy Digest, 1972) for annealed tubing is 772 MPa, well below the

yield strength of material cold worked to 25%.

## RESULTS AND DISCUSSION

The residual stress and cold work distributions produced by reaming the inside diameter surface of the Alloy 600 sleeves were measured on a separate portion of a sleeve which was not welded. The residual stress and (420) peak width distributions obtained as functions of depth in the drawn and reamed areas are shown in Fig. 4.

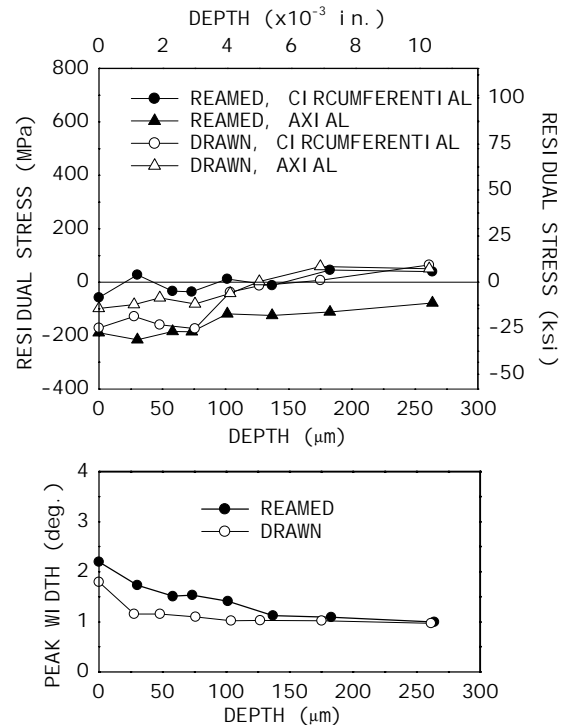


**Fig. 4** - Baseline subsurface axial and circumferential residual stress and (420) peak width distributions for drawn and reamed Inconel 600 sleeve removed from service.

The stress distributions remaining after the initial tube drawing operation are compressive in both the circumferential and axial directions, less than -200 MPa, from the surface to a depth of nominally 125  $\mu\text{m}$ . Following reaming, the axial direction is more compressive to the maximum depth examined, and the circumferential direction was found to be nearly stress free. The (420) peak width distributions shown at the bottom of Fig. 4 reveal that the reaming operation induces more cold work, to a deeper depth, than the initial drawing. The amount of cold work, estimated from the empirical curve shown in Fig. 2, is nearly 25% at the inside surface of the drawn tube, and over 50% after reaming, as shown in the top of Fig 5. Deformation from reaming extends to 150  $\mu\text{m}$  beneath the surface. The corresponding yield strength,

estimated from the true stress-strain curve in Fig. 3, is on the order of 900 to 1000 MPa at the deformed surface of the reamed areas. The yield strength drops rapidly to near the nominal bulk value of 443 MPa at a depth of only 25  $\mu\text{m}$  for the drawn surface, but remains well above the nominal yield strength to a depth of approximately 150  $\mu\text{m}$ , for the reamed surface, diminishing nearly linearly with depth.

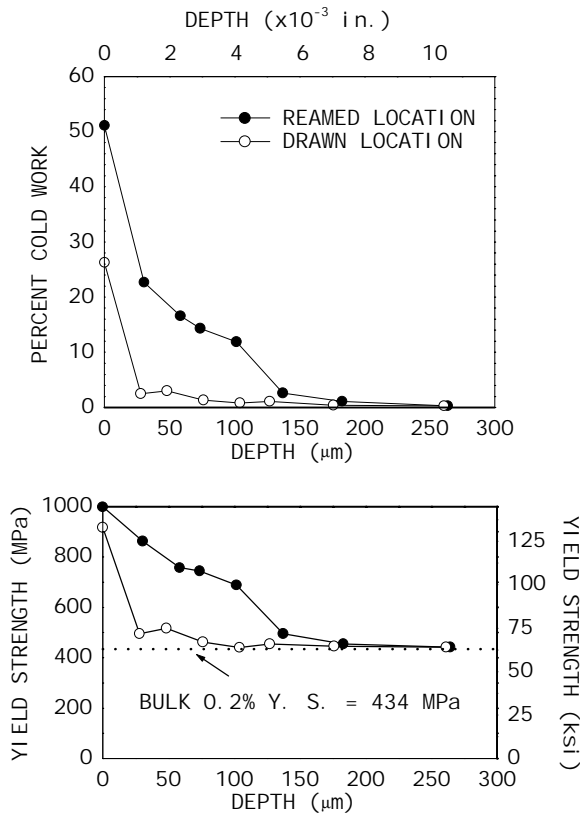


**Fig. 5** - Subsurface percent cold work (equivalent accumulated true plastic strain) and corresponding yield strength distributions for baseline drawn and reamed locations on Alloy 600 sleeves removed from service.

The complex cold work distributions, measured on the inside surface of the welded sleeve are presented in Fig. 6. The reamed surface layers are the most deformed. The reamed surface, remote from the weld, is deformed nearly 60%, comparable to the surface results prior to welding, shown in Fig. 5. An increase in the amount of cold work in the reamed area, attributed to additional cold working caused by weld shrinkage at the edge of the HAZ, is evident at

virtually all depths between approximately -20 and -15 mm. At a depth of 254  $\mu\text{m}$ , the material is free of cold work in the reamed zone beyond approximately -30 mm, and in the original drawn tubing beyond approximately 25 mm. All layers deeper than nominally 25  $\mu\text{m}$  appear to be fully annealed in the center of the HAZ. Weld shrinkage has deformed the Alloy 600 nominally 5% in the regions 5 to 25 mm on either side of the fusion line. The inside surface still retains in excess of 40% cold work at the center of the HAZ, indicating only depths greater than 25  $\mu\text{m}$  were fully annealed during welding to the outside surface of the sleeve.

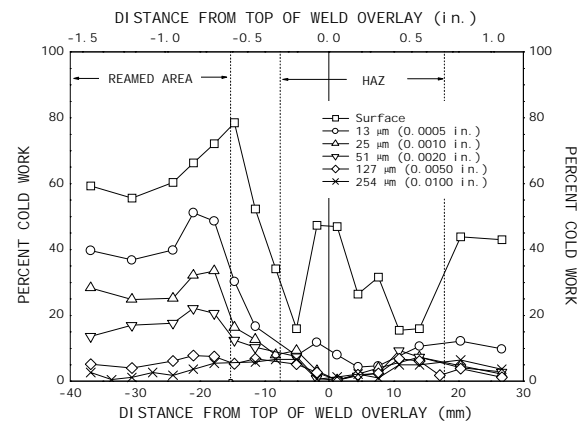


**Fig. 6** - Variation in degree of cold work (equivalent accumulated true plastic strain) with axial displacement and depth in the HAZ and machined regions of the low angle side of 50 deg. Alloy 600 J-weld mockup.

The yield strength distributions, estimated from the percent cold work and the true stress-strain curve, are presented in Fig. 7. Because the degree of cold work produced by machining exceeded the range of the uniaxial tension true stress-strain curve, yield strengths in excess of nominally 900 MPa have been extrapolated. The yield strength in the reamed area outside the HAZ exceeds the nominal bulk engineering yield stress of 443 MPa at all depths from the surface down to 127  $\mu\text{m}$ . After the severe deformation produced by reaming, the surface and 13  $\mu\text{m}$  depths in the HAZ are capable of supporting residual stresses well in excess of the published engineering yield strength of the material, because these depths were not fully annealed during welding. The yield strength at the surface of the drawn region, beyond 20 mm, is significantly increased from the surface to a depth of 13  $\mu\text{m}$ .

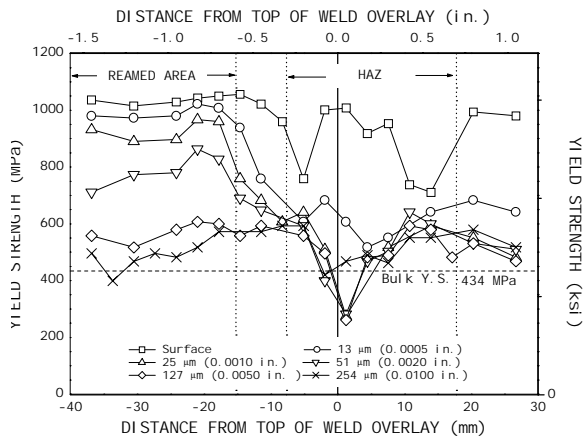


**Fig. 7** - Variation in yield strength with axial displacement and depth in the HAZ and machined regions of the low angle side of the 50 deg. Alloy 600 J-weld mockup, relative to the bulk yield strength.

The axial and circumferential residual stress distributions are presented as functions of axial position and depth in Fig. 8 and 9, respectively. As a consequence of the complex thermal-mechanical history of the weld fusion region, the residual stress distributions are also quite complex. The most tensile residual stresses were produced in the reamed area adjacent to the HAZ. This region is close enough to the fusion zone for significant weld shrinkage to pull the cold worked surface into tension, but too remote for significant annealing during welding. The axial stress rises to +650 MPa tension at approximately -15 mm. The axial tension diminishes rapidly with depth, but exceeds the stress corrosion threshold in the reamed area nearest the HAZ at all depths examined. The increase in axial tension with increasing depth in the reamed region between -30 and -40 mm is attributed to distortion of the sleeve caused by weld shrinkage. The axial residual stresses in the HAZ are beneath the stress corrosion threshold, or even entirely compressive, at all depths examined approximately 8 mm into the block. The axial stresses return to tension, nearly uniform with depth, in the unreamed area beyond nominally 18 mm.

The circumferential residual stress distributions, shown in Fig. 9, are tensile, generally in excess of the SCC threshold, and highest just beneath the surface at 13 μm in the reamed area adjacent to the HAZ. The Alloy 600 is in tension from -30 to +18 mm, and most uniformly in tension at the maximum depth of 250 μm examined. The circumferential stress is on the order of the bulk yield strength of the material at the 254 μm depth between -30 and +12 mm. The nearly uniform deep circumferential tension is attributed to weld shrinkage expanding the sleeve radially. The circumferential stress distributions are entirely

compressive at all depths in the unreamed material beyond a distance of 20 mm into the block.

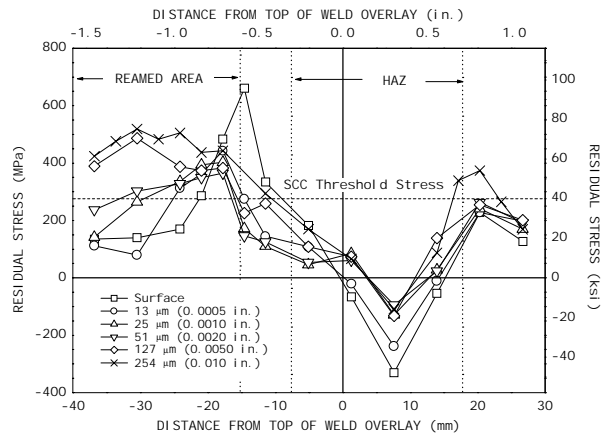


**Fig. 8** - Variation in axial residual stress with axial displacement and depth through the HAZ and machined regions on the low angle side of the 50 deg. J-weld Alloy 600 mockup.

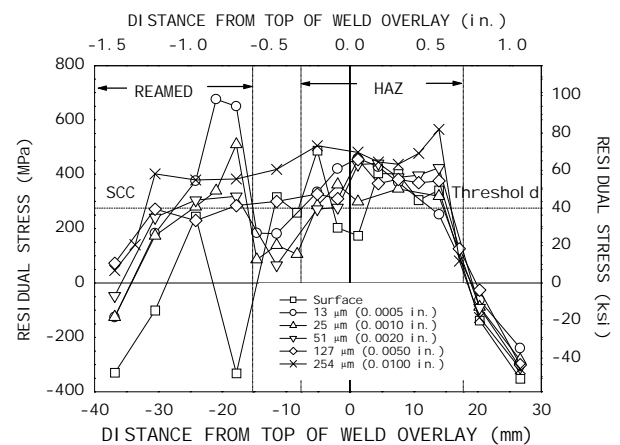


**Fig. 9** - Variation in circumferential residual stress with axial displacement and depth on the low angle side of the 50 deg. Alloy 600 J-weld mockup showing stresses in excess of the SCC threshold.

## CONCLUSIONS

This study provides an excellent example of the use of XRD to determine the complex residual stress and material property distributions produced by a combination of machining and welding. Several conclusions appear to be supported by the results obtained:

- The combination of prior machining and weld shrinkage can produce residual stress and yield strength distributions which vary rapidly with

depth and position, with very localized tensile areas susceptible to SCC.

- The cold work produced by the combination of machining and weld shrinkage of austenitic alloys alters the mechanical properties, specifically the yield strength, of the deformed surface layers. The yield strength of the deformed material can be well in excess of the bulk yield for the alloy, and is therefore capable of supporting residual stresses correspondingly higher.
- Alloy 600 may be cold worked over 50% by machining processes such as reaming, and at least an additional 5% by weld shrinkage in a constrained geometry, resulting in yield strengths over 900 MPa on the reamed surface and 600 MPa adjacent to the HAZ in material not previously deformed by machining.
- The cold work due to weld shrinkage is accumulative in the reamed area adjacent to the HAZ, being additive to the prior cold work produced by machining.
- The residual stresses developed by welding depend upon the yield strength and residual stress distributions produced by prior machining. Therefore, minimizing the cold working and residual stress developed by prior machining may be beneficial.

## ACKNOWLEDGEMENTS

The authors acknowledge the assistance of ABB Combustion Engineering for preparing the samples, providing the true stress-strain data and many helpful discussions, and Dr. R. S. Pathania of EPRI for support for the sample fabrication and the initial investigation of J-weld residual stresses under EPRI contract no. RP3223-02.

## REFERENCES

1. Alloy Digest, 1972, Inconel Alloy 600 Spec. Sheet Ni-176, Eng. Alloys Dig., Upper Montclair, NJ.
2. Cullity, B.D., 1978, Elements of X-ray Diffraction, 2nd ed., Addison-Wesley, Reading, MA, pp. 447-476.
3. Gorman, J.A., 1986, "Status and Suggested Course of Action for Nondenting-Related Primary-Side IGSCD of Westinghouse-Type Steam Generators," EPRI, Report MP-4594-LD.
4. Hall, J.F., and Scott, D.B., 1989, "Destructive Examination of Pressurizer Heater Sleeves from Calvert Cliffs Unit 2," Report CE-NPSD-577.
5. Hall, J.F., Molkenhuth, J.P., and Prev y, P.S., 1993, "XRD Residual Stress Measurements on Alloy 600 Pressurizer Heater Sleeve Mockups," Proceedings of the Sixth International Symposium on Environmental Degradation of Materials in Nuclear Power Systems-Water Reactors, TMS, ANS, NACE, San Diego, CA, pp. 855-861.
6. Hall, J.F., Molkenhuth, J.P., Prev y, P.S., and Pathania, R.S., 1994, "Measurement of Residual Stresses in Alloy 600 Pressurizer Penetrations," Conference on the Contribution of Materials Investigation to the Resolution of Problems Encountered in Pressurized Water Reactors, Societe Francaise d'Energie Nucleaire, Paris.
7. Hilley, M.E., ed., 1971, "Residual Stress Measurement by X-Ray Diffraction," SAE J784a, Society of Auto. Eng., Warrendale, PA.
8. Noyan, I.C., and Cohen, J.B., 1987, Residual Stress Measurement by Diffraction and Interpretation, Springer-Verlag, New York, NY.
9. Prev y, P.S., 1977, "A Method of Determining Elastic Properties of Alloys in Selected Crystallographic Directions for X-Ray Diffraction Residual Stress Measurement," Adv. in X-Ray Analysis, Vol. 20, Plenum Press, New York, NY, pp. 345-354.
10. Prev y, P.S., 1981, "Surface Residual Stress Distributions in As-Bent Inconel 600 U-Bend and Incoloy 800 90-Degree Bend Tubing Samples," Workshop Proceedings: U-Bend Tube Cracking in Steam Generators, EPRI, Palo Alto, CA, pp. 12-3 to 12-9.
11. Prev y, P.S., 1986a, "X-Ray Diffraction Residual Stress Techniques," Metals Handbook, Vol 10, ASM, Metals Park, OH, pp. 380-392.
12. Prev y, P.S., 1986b, "The Use of Pearson VII Functions in X-Ray Diffraction Residual Stress Measurement," Adv. in X-Ray Analysis, Vol. 29, Plenum Press, New York, NY, pp. 103-112.
13. Prev y, P.S., 1987, "The Measurement of Residual Stress and Cold Work Distributions in Nickel Base Alloys," Residual Stress in Design, Process and Material Selection, ASM, Metals Park, OH, pp. 11-18.